Heliyon 5 (2019) e01988

Contents lists available at ScienceDirect

Heliyon

journal homepage: www.heliyon.com

Effect of NaCl on the properties of sulphamic acid single crystals

J. Arumugam [a,b], N. Suresh [a,b], M. Selvapandiyan [a,*], S. Sudhakar [c], M. Prasath [a]

[a] Department of Physics, Periyar University PG Extension Centre, Dharmapuri, 636 705, Tamil Nadu, India
[b] Department of Physics, Sri Vidya Mandir Arts and Science College, Uthangarai, 636 902, Tamil Nadu, India
[c] Central Electrochemical Research Institute, Karaikudi, 630 003, Tamil Nadu, India

ARTICLE INFO

Keywords:
Materials science
Crystal growth
Optical properties
Z-scan technique
Laser damage threshold
Thermal properties

ABSTRACT

Single crystals of pure and NaCl doped sulphamic acid (SA) were grown by slow evaporation method at room temperature. The lattice parameters and structure were determined by using single crystal and powder X-ray diffraction analyses. The presence of dopant in the SA lattice was affirmed by EDAX analysis. UV-Vis spectra show maximum transmittance in the visible region. The band gap energies were found to be 6.06 eV and 5.70 eV for pure and NaCl doped SA crystals respectively. From the PL specta the emission were observed at 335 and 424 nm for pure and 340 and 428 nm for doped SA crystal. The thermal stability of the grown crystals were analyzed by thermogravimetric and differential thermal analysis (TGA/DTA) and revealed that the grown crystals were thermally stable up to 331°C and 334°C for pure and NaCl doped SA. Vickers microhardness study reveals that the hardness of the crystals is increase with increasing load. The photoconductivity study shows that the grown crystals are negative photoconductive nature. The Laser Damage Threshold (LDT) indicates the grown crystals have good resistance to laser radiation than a standard Potassium dihydrogen phosphate (KDP) crystal. The Z-scan technique was employed to determine the nonlinear refractive index, nonlinear optical absorption and third order nonlinear optical (TONLO) susceptibility of the grown crystals using He–Ne laser.

1. Introduction

Recently, the nonlinear optical materials with enhanced third order nonlinear optical susceptibility χ^3 have been used in wide range of applications such as 3D optical memory, optical switching, optical modulating, laser technology, optical communication, optical storage technology and optical limiting etc,. In the few decades, many organic and inorganic materials have been developed to cover the possible applications in Ultraviolet (UV), near and far-infrared (IR) wavelength regions [1, 2, 3, 4, 5, 6, 7, 8]. Inorganic crystals have high laser-induced damage threshold energy compared to organic crystals, the materials with high nonlinear absorption, ultra fast response time and large third order optical nonlinearity are essential in two photon laser scanning microscopy, phase conjugation, low intensity lasers and microfabrication [9]. It was observed from literature that inorganic NLO materials have excellent mechanical and thermal properties, but possess relatively modest optical nonlinearity because of the lack of extended π-electron delocalization [10, 11]. Doping of metal ions and rare earth ions in the inorganic single crystal shows remarkable industrial applications in executing the efficient optical properties [3, 22]. The zwitter ionic nature of the molecule favours crystal hardness [12]. Sulphamic acid [H_2NSO_3H] is a strong inorganic acid, when mixed with water it exhibits zwitter ionic nature [13]. Sulphamic acid belongs to orthorhombic structure and the relevant lattice parameters are a = 8.078 (Å), b = 8.116 (Å) and c = 9.268 (Å) [14]. Among all amino acids, sulphamic acid and derivatives exhibited large industrial applications [15, 16, 17]. Dopant play vital role to enhance the physical properties of single crystals. Few authors reported the effect of dopants on the growth and physical properties of inorganic SA single crystal [3, 14, 15, 18, 19, 20, 21]. From the literature survey it was observed that addition of metal enhances the optical, ferroelectric and dielectric properties of the crystals [15]. Incorporation of small amount of impurities in the form of cationic dopant K^+ and Na^+ increases the growth rate, physical and chemical properties of the crystals [17]. Thaila et al. reported the effect of NaCl and KCl (0.1 mol %) doping on the growth of SA crystal [20]. The present paper describes and discusses the experimental results concerning the influence of NaCl (1 mol%) ion on sulphamic acid. In this work, we report the growth and characterization of pure and NaCl doped sulphamic acid crystal, also the effect of dopant with sulphamic acid is discussed in detail. The structure, optical properties, microhardness, dielectric, thermal stability, laser damage threshold and photoconductive properties of the grown pure and doped SA crystals were reported. To the best of our

* Corresponding author.
E-mail address: mselvapandiyan@rediffmail.com (M. Selvapandiyan).

https://doi.org/10.1016/j.heliyon.2019.e01988
Received 5 December 2018; Received in revised form 28 March 2019; Accepted 18 June 2019
2405-8440/© 2019 The Authors. Published by Elsevier Ltd. This is an open access article under the CC BY-NC-ND license (http://creativecommons.org/licenses/by-nc-nd/4.0/).

knowledge, no authors were discussed the third order nonlinear optical property (TONLOP) on SA and NaCl doped SA. Hence, the authors analysed the third order nonlinear optical property (TONLOP) of NaCl doped SA crystals using Z-scan technique and the results were reported in this articles.

2. Experimental

2.1. Crystal growth

Pure and 1 mol % of NaCl doped sulphamic acid single crystals were grown by slow evaporation technique at ambient temperature. The sulphamic acid [H_2NSO_3H], sodium chloride [NaCl] and deionized water were used for the crystal growth. The calculated amount of sulphamic acid salt was taken in a clean glass vessel and dissolved in 100 ml deionized water. The solution was continuously stirred using magnetic stirrer to get homogeneous solution. After 3 hours, the saturated homogeneous solution was filtered by Whatmann filter paper. The filtered solution was kept in a dust free atmosphere for evaporation. Well defined, colourless and good transparency crystal of dimension up to 12 $\times$ 7 $\times$ 4 mm^3 was collected at the end of 25th day. Again saturated solution of sulphamic acid was prepared and then 1 mol % of NaCl solution was added to sulphamic acid solution and stirred well for 4 hours to get homogeneous solution. It was filtered by Whatmann filter paper. The good quality of 1 mol % of NaCl doped sulphamic acid crystals were harvested with dimension of 13 $\times$ 13 $\times$ 4 mm^3 (After 35 days). The photograph of grown pure, 1 mol % of NaCl doped sulphamic acid single crystals and theoretical XRD pattern were shown in Fig. 1 (a), (b) and (c) respectively.

2.2. Characterization techniques

The single crystal X-ray diffraction studies were carried out using Enraf-Nonius CAD4 diffractometer with Mo-Kα radiation (0.71073Å). The powder X-ray diffraction (PXRD) analyses were performed using X'Pert pro analytical diffractometer with Cu-Kα radiation (1.54060 Å) and operated at 50 kV. The sample was scanned from 10° to 80° at ambient temperature. The PXRD pattern of the grown crystals was indexed using the celn software. The Energy Dispersive X-ray analysis (EDAX) spectrum was recorded using EDS-BRUKER nano, GmbH, D-12489, Germany,

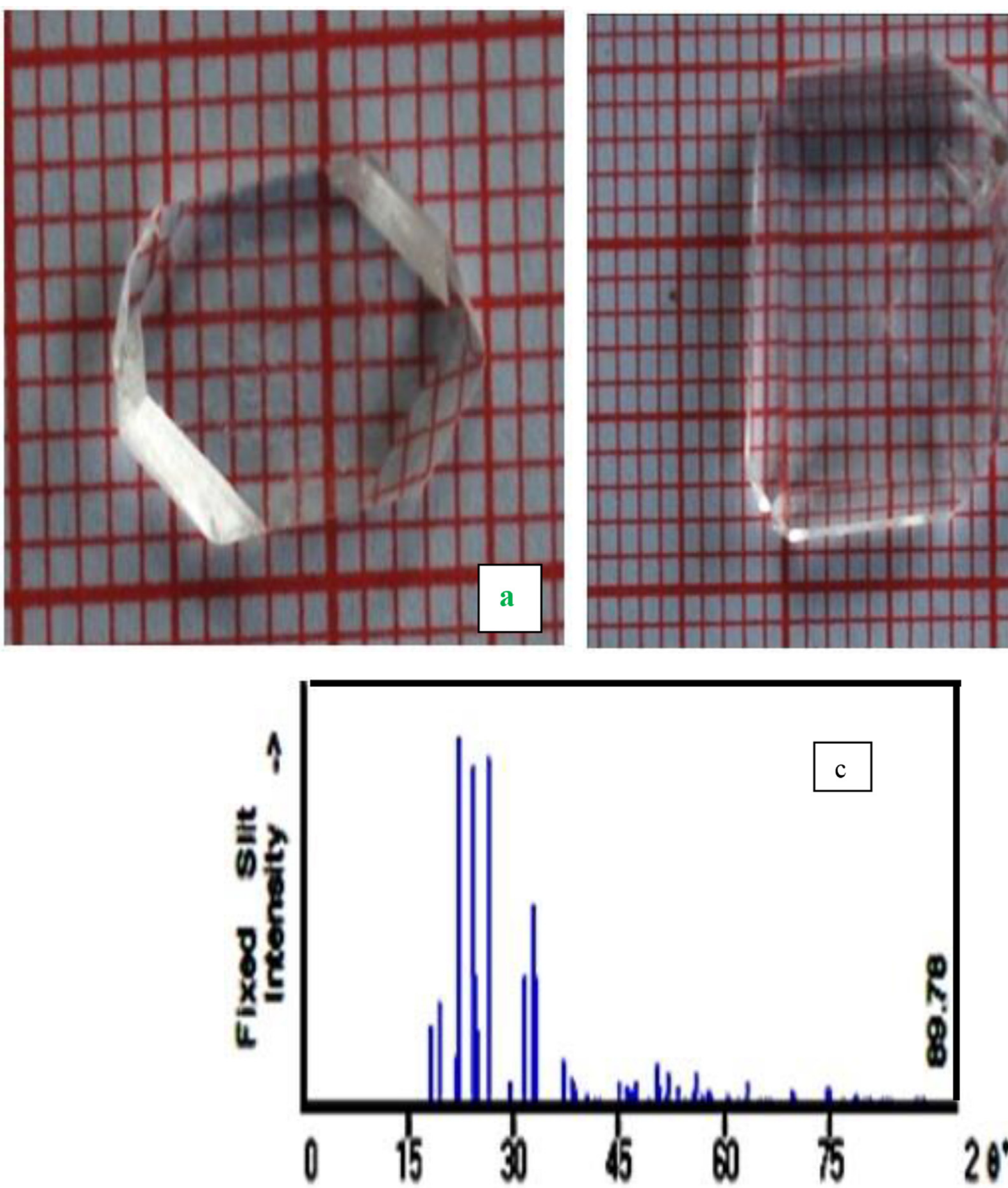

Fig. 1. As grown Crystals of SA: (a) Pure, and (b) 1 mol. % NaCl doped SA; (c) Theoretical XRD pattern of SA.

accelerating voltage 0–30 V. The optical spectra of crystals were recorded using Lambda 35 model in the wavelength range from 190 nm to 700 nm with the thickness of 2 mm. The photoluminescence of the grown crystals was carried out using Perkin Elmer-LS Luminescence spectrometer at room temperature. The emission spectrum was recorded in the range of 200 nm–600 nm. Thermogravimetric analysis and differential thermal analysis were carried out using SEIKO TGA/DTA 6200 model at a heating rate of 20 °C/min in nitrogen atmosphere. The microhardness test was carried out in HM-2TV model tester. The photoconductivity studies were carried out using KEITHLEY PICOMETER in the presence of DC electric field at ambient temperature. The laser damage threshold measurements were carried out using Q-switched Nd: YAG laser (λ = 1064 nm) with 10 ns pulse width and repetition rate of 10 Hz. A laser beam of 1mm was used to irradiate on the well-polished sample (3 mm) surface with 15 cm focal length lens. The Z-scan technique was carried out using a solid state laser of the wavelength of 632.8 nm.

3. Results and discussion

3.1. X-ray diffraction studies

From single and powder XRD analyses it was confirmed that the grown both pure and 1 mol % of NaCl doped sulphamic acid crystals belong to orthorhombic crystal system [14]. The obtained lattice parameter of grown crystals is shown in Table 1. The powder X-ray diffraction pattern of grown crystals was shown in Fig. 2. The pure and 1 mol % of NaCl doped SA crystals have shown sharp peaks. The diffraction intensity of the 1 mol % of NaCl doped SA is higher than the pure SA crystal, which may be due to the incorporation of Na^+ ion into the SA lattice. The PXRD analysis also reveals that the presence of Na^+ ion did not alter the basic crystal structure of SA but slight variation in lattice parameters due to Na^+ ion in sulphamic acid lattice.

3.2. Energy dispersive X-ray analysis (EDAX)

The chemical composition of grown pure and 1 mol % of NaCl doped SA crystals were obtained from energy dispersive X-ray spectra. The presence of metal Na^+ ions in the SA crystal was confirmed. The recorded EDAX spectra of grown crystals were shown in Fig. 3 (a & b). From the characteristic peaks, the presence of Sulphur, Nitrogen, Oxygen, Sodium and Chlorine were detected.

3.3. UV-visible analysis

The recorded absorption spectrum of grown crystals was shown in Fig. 4. The lower cut off wavelength of grown single crystals were 207 nm and 243 nm for pure and 1 mol % of NaCl doped sulphamic acid single crystals and percentage of absorption is high for doped single crystal in comparison with pure sulphamic acid and it could be due to the influence of dopant Na^+ ion in SA crystal lattice [23, 24]. The Tauc's plot analysis were carried out to find the energy band gap values and shown in Fig. 5. The obtained optical band gap energies of pure and 1 mol % of NaCl doped SA were 6.06 eV and 5.70 eV respectively. The results confirmed

Table 1
Lattice parameters of the grown crystals.

Lattice parameters	Reported values [12]	Undoped SA	1 mol% of NaCl added SA
a (Å)	8.078	8.063	8.074
b (Å)	8.116	8.099	8.091
c (Å)	9.268	9.208	9.239
α (deg)	90	90	90
β (deg)	90	90	90
γ (deg)	90	90	90
Volume (A3)	607.6	601.3	603.6
System	orthorhombic	orthorhombic	orthorhombic

that the pure and NaCl doped SA belong to the category of insulating materials.

3.4. Photoluminescence analysis

Photoluminescence spectroscopy is the standard technique for characterizing defects, vacancies and other imperfections existing in the crystals [25, 26]. The emission spectrum was recorded between 200 nm to 600 nm (Fig. 6). The intense emission bands are observed 335 nm, 424 nm for pure and 340 nm, 428 nm for 1 mol % of NaCl doped SA crystal. The emission bands were observed in the UV region at 335 nm and 340 nm due to the electronic transition π-π* [27, 28]. The peak at 424 nm is associated with indirect transitions in the Pristine Sulphamic acid crystal. As NaCl is added to Sulphamic acid, the emission band was slightly higher shifted i.e. 428 nm, which shows a blue emission.

3.5. Thermal analysis

The TGA-DTA curves of grown crystals were shown in Fig. 7. From the TGA curve, the pure and 1 mol % of NaCl doped sulphamic acid crystals are thermally stable up to 331° C and 334° C and the weight loss started above this temperature. The weight loss may be liberation of one molecule of nitrogen oxide and one molecule of sulphur dioxide [29, 30]. From DTA curve, the first endothermic peaks at 251° C and 250° C reveal the melting point of the pure and 1 mol % of NaCl doped SA crystals respectively. Furthermore, a complete decomposition or volatilization was also observed at or after 450° C with the appearance of second endothermic peaks. The sharpness endothermic peaks represent the melting point of the crystals.

3.6. Vicker's microhardness studies

The applications of the crystals are not only depended on good optical performance but also with good mechanical behaviour [31, 32]. The static indentations were carried out using a Vicker's indenter for varying loads. For each load P, several indentations were made and the average value of diagonal length d was measured to calculate the microhardness of the crystals. Vicker's microhardness number was determined using with the relation:

$$H_v = \frac{1.8544P}{d^2} \tag{1}$$

For a static indentation test with load P varying from 25, 50, 100 and 200 g, the plot between load and hardness number is shown Fig. 8. From the plot, it was clearly seen that the hardness number increased with increase in load up to 200 g no cracks had been observed. The presence of dopant Na^+ ion is played a vital role in enhancing the hardness property of the SA crystal. Similar behaviour was observed for various metal ions such as Cu^{2+}, Mn^{2+} and Ni^{2+} doped SA crystals [16]. A plot between log P and log d (Fig. 9) found to be a straight line. The relation connecting the applied load and diagonal length d of the indenter was provided by Mayer's law:

$$P = ad^n \tag{2}$$

where, P is the load in kg, d is the mean diagonal length and n is the Mayer's index. According to Onitsch, if n values lied between 1 and 1.6 for hard materials and it was more than 1.6 for soft materials category [33, 34, 35]. The obtained value for pure and 1 mol % of NaCl doped SA were 2.018 and 2.233, respectively. The results indicated that the pure and 1 mol % of NaCl doped SA crystals were considered to be soft material nature.

3.7. Photoconductivity measurement

Photoconductivity of a material depends on the several functions such

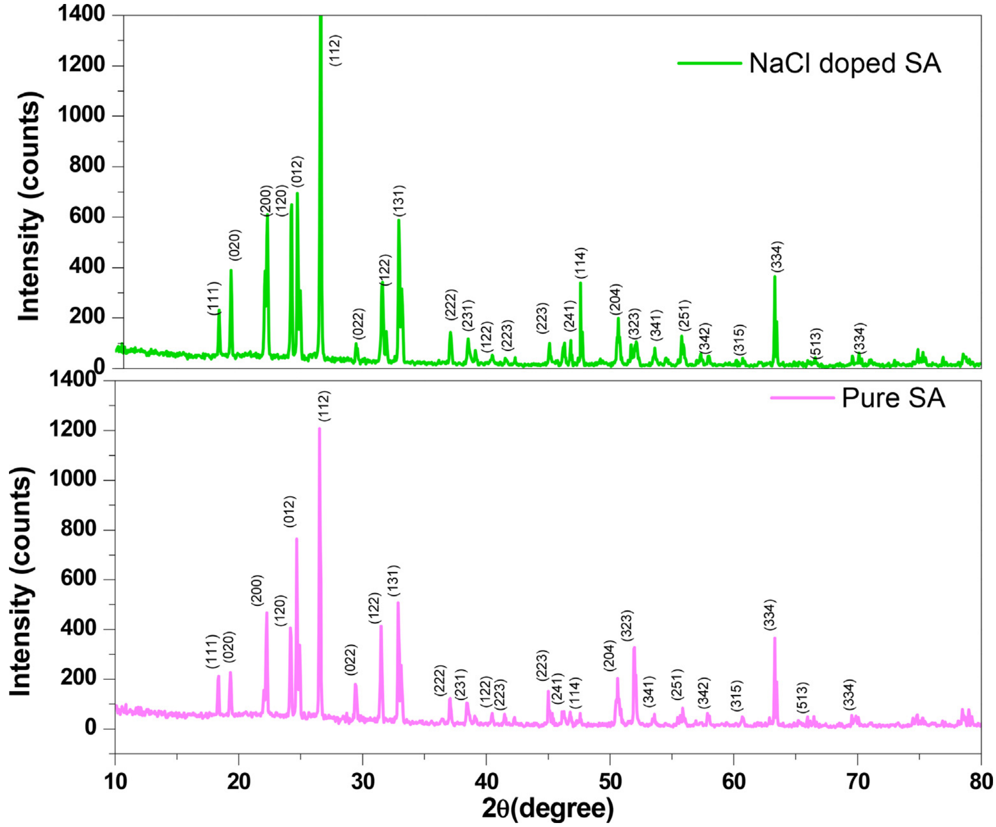

Fig. 2. Powder X-ray diffraction patterns of pure and NaCl doped SA crystal.

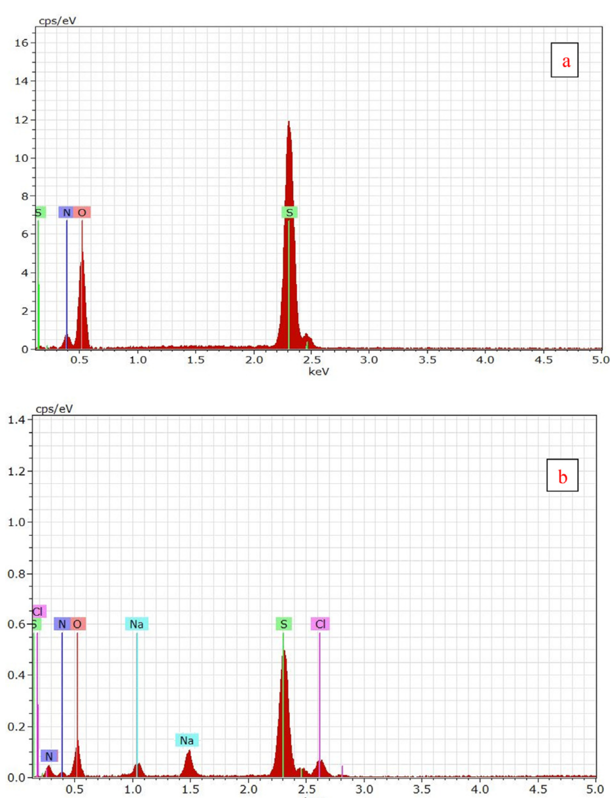

Fig. 3. EDAX spectrum for (a) Pure, and (b) NaCl doped SA crystal.

as temperature, applied voltage, intensity of light and so on [35, 36]. The photo current of the grown crystals were illuminated with the halogen lamp [100 W]. The plot of photo current and dark current are shown in Fig. 10. The photo current is found to be less than that of the dark current, which indicates that both crystals exhibit negative photoconductivity nature of the material. The photo and dark current of pure and 1 mol % of NaCl doped SA single crystals were increased linearly with the applied voltage. The negative photoconductivity exhibited by the sample may be due to the presence of minimum charge carriers in the presence of radiation.

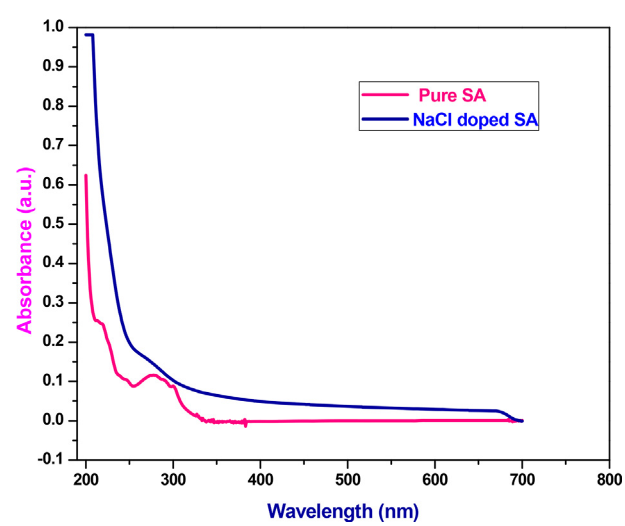

Fig. 4. Absorption spectra of Pure and 1mol. % NaCl doped SA crystal.

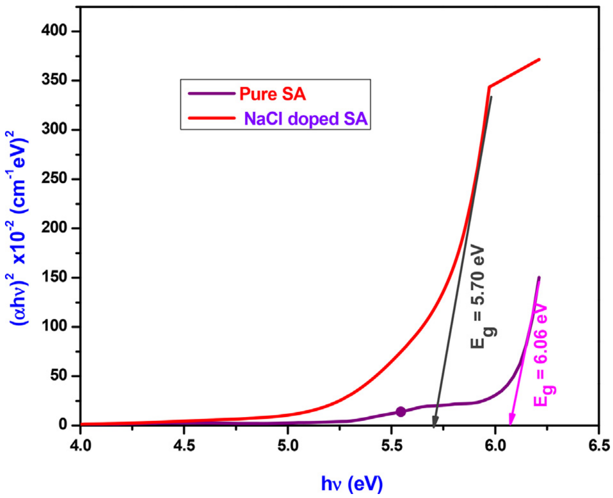

Fig. 5. Tauc's plot for pure and 1mol. % NaCl doped SA crystal.

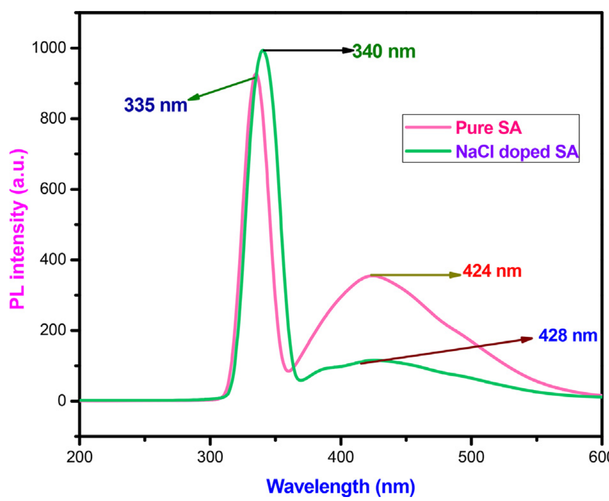

Fig. 6. Photoluminescence spectra of Pure and 1 mol. % NaCl doped SA crystal.

3.8. *Laser damage threshold (LDT) measurements*

The laser damage threshold of an optical material was an important parameter to measure its applicability [37, 38], the ability of an optical crystal under laser irradiation was measured by laser damage threshold studies. It is considered as an essential factor for laser assisted applications. For nonlinear optics and laser applications, the laser-induced damage threshold value was an important criterion because it gives the limit of performance in the optical device [39]. The different laser light energy was irradiated on the surface of grown crystals. The energy value was reached at 57.5, 89 and 139 mJ. At energy, a clear visible image occurred for KDP, pure SA and 1 mol % of NaCl doped SA crystals. During the laser irradiation, the input laser energy density was recorded using power meter. The surface damage threshold of the grown crystals was calculated using the relation – 3 [39, 40, 41].

$$\text{Power density } P_d = \frac{E_p}{\tau\pi(\omega_0)^2} \tag{3}$$

where, E_p is the input pulse energy (mJ) of the laser beam when microscopic damage appeared, τ is the pulse width (ns) and ω_o is the radius of beam waist. The calculated laser damage threshold value of KDP, pure and 1 mol % of NaCl doped SA crystals are 17.72, 27.42 and 42.83 GW/cm^2, respectively. The calculated laser damage threshold value of 1 mol % of NaCl doped SA crystal is higher than the pure and KDP crystals. This high LDT value suggest that NaCl doped SA crystal might find applications in the development of laser supported non-linear optical devices.

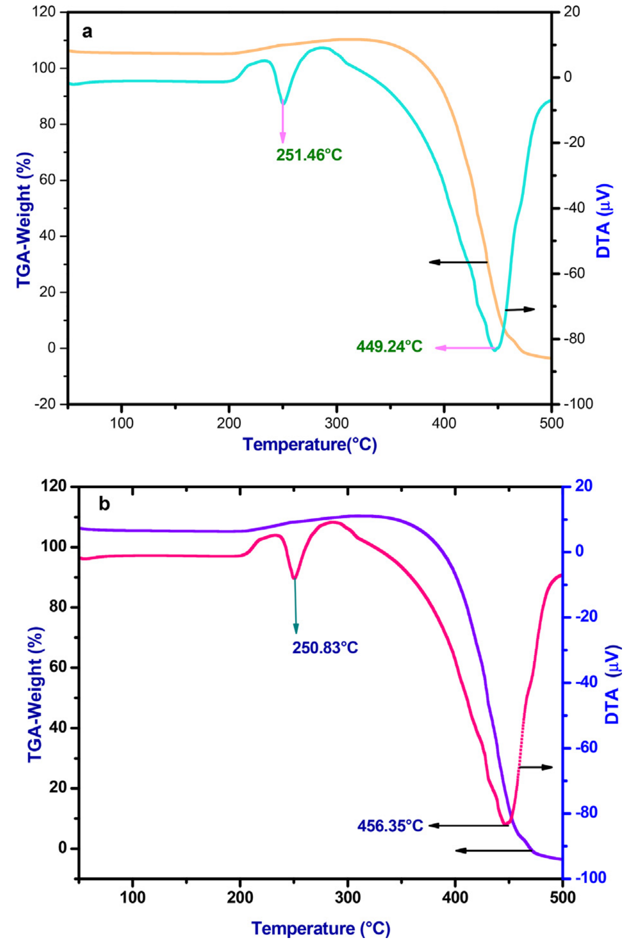

Fig. 7. TGA-DTA curve of (a) pure SA and (b) 1 mol. % NaCl doped SA crystal.

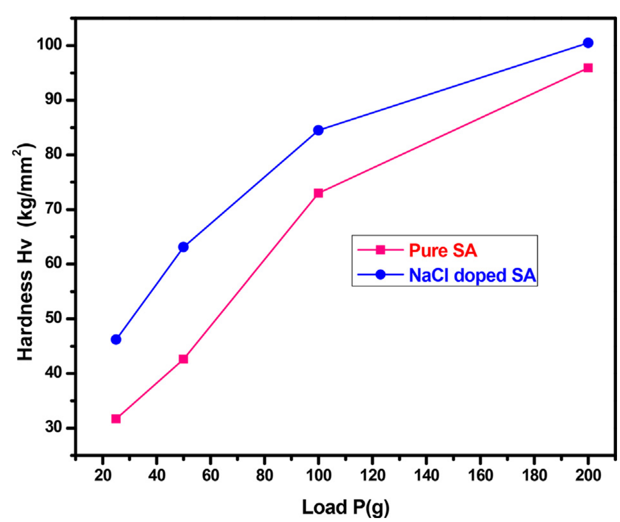

Fig. 8. Load (P) vs Hardness number for Pure and 1 mol. % NaCl doped SA crystal.

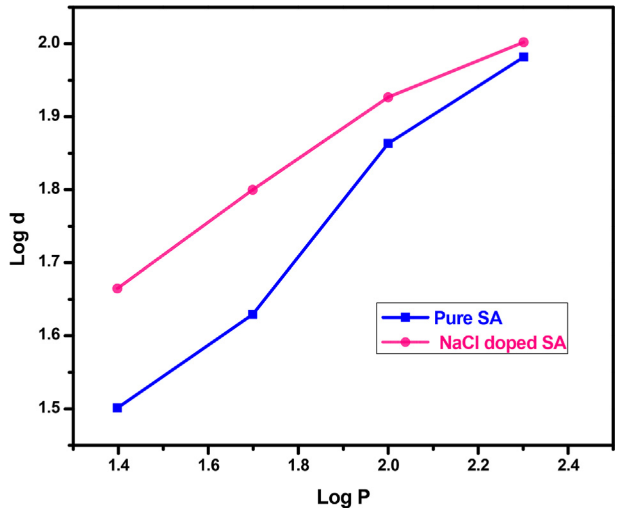

Fig. 9. Log P vs Log d for Pure and 1 mol. % NaCl doped SA crystal.

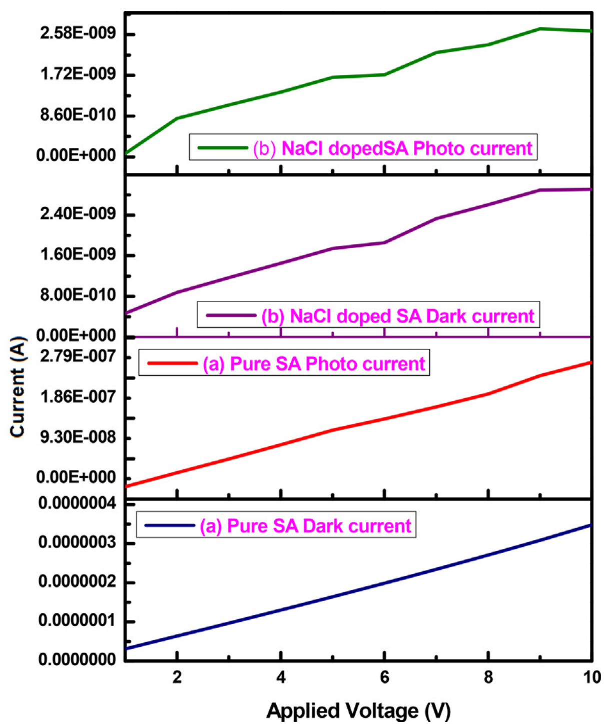

Fig. 10. Photoconductivity spectra of grown crystals of SA: (a) Pure, and (b) 1 mol. % NaCl doped SA crystal.

3.9. Third order NLO properties

The Z-scan technique is an important and sensitive technique to calculate the third order nonlinear optical parameters [42, 43, 44, 45]. Using the Z-scan technique, the open and closed aperture Z-scan spectra, the nonlinear absorption coefficient and nonlinear optical refraction were calculated. Figs.11 and 12 shows the open and closed aperture Z-scan curves of the pure and 1 mol % of NaCl doped SA crystals. To determine the third order nonlinear susceptibility there are the two main parameters are needed. One is the value of nonlinear absorption coefficient and other is sign and the magnitude of nonlinear refraction. From the open aperture Z-scan spectra the nonlinear absorption coefficient was calculated. However, from the closed aperture Z-scan spectrum with pre focal valley and post focal peak indicates a self focusing process. It is a positive sign for nonlinear refraction [45]. To find out the nonlinear

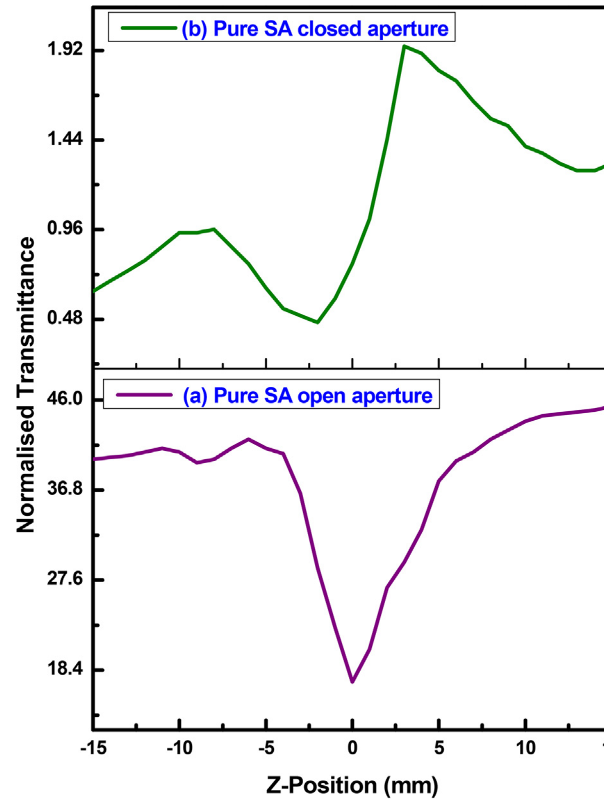

Fig. 11. a and b. Open and Closed aperture Z-scan curves of grown SA crystal.

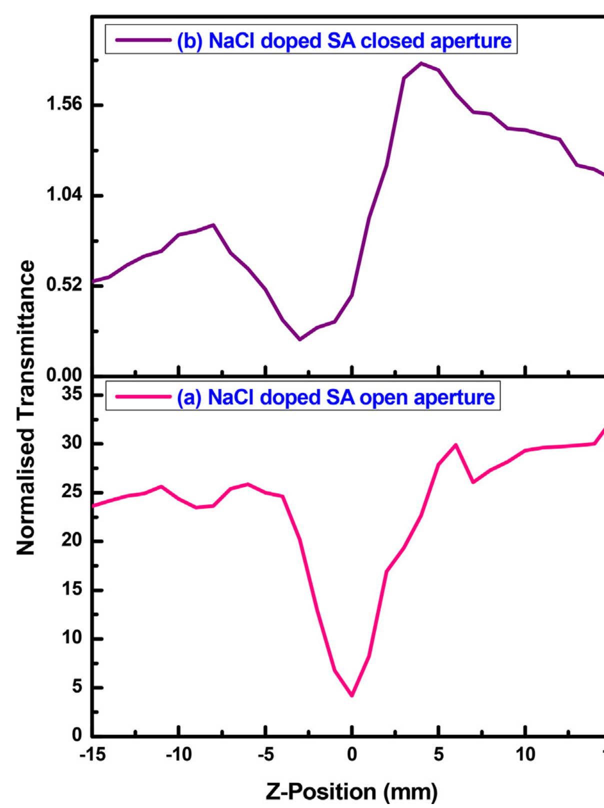

Fig. 12. a and b. Open and Closed aperture Z-scan curves of grown 1 mol. % NaCl doped SA crystal.

refractive index of grown pure and 1 mol % of NaCl doped SA crystals, the difference of the normalized peak and valley transmissions (ΔT_{p-v}) was calculated using the relation:

$$|\Delta\varphi| = \frac{\Delta T_{p-v}}{0.406(1-S)^{0.25}} \quad (4)$$

where, $\Delta\varphi$ is the axis phase shift at the focus, S is the linear transmittance aperture. It can determine the expression:

$$S = 1 - \exp\left(-2r_a^2/\omega_a^2\right) \quad (5)$$

where r_a is the radius of the capture (2 mm) and ω_a is the beam radius at the capture (3.3 mm). The third order nonlinear refractive index was calculated using the relation

$$n_2 = \frac{\Delta\varphi}{KI_0L_{eff}}\left(m^2/W\right) \quad (6)$$

where, K is the wavenumber, I_0 is the intensity of the laser beam at the focus and L_{eff} is the effective thickness of the materials. The nonlinear absorption coefficient was determined using an open aperture. The value of β will be the positive for two or multi photon absorptions and negative for saturable absorption and the β value can be evaluated using the expression:

$$\beta = \frac{2\sqrt{2\Delta T}}{I_0L_{eff}}(m/W) \quad (7)$$

where, K is the wave number it value can be determined using $K = 2\pi/\lambda$, ΔT is the peak value at the open aperture Z-scan curve and I_o is the intensity of the laser at the focus (z = 0). The effective thickness of the sample was calculated by using the relation:

$$L_{eff} = [1 - \exp(-\alpha L)]/L \quad (8)$$

where, α is the linear absorption coefficient and L is the thickness of the sample. The effective thickness was found to be 0.6 mm. The real and imaginary parts of the third order nonlinear optical susceptibility were found out by the relations:

$$R_e\chi^{(3)}(esu) = 10^{-4}\varepsilon_o c^2 n_o^2 n_2/\pi\left(cm^2/W\right) \quad (9)$$

$$I_e\chi^{(3)}(esu) = 10^{-2}\varepsilon_o c^2 n_o^2 \lambda\beta/4\pi^2\left(cm^2/W\right) \quad (10)$$

where, ε_o is the vacuum permittivity (8.854 × 10^{-12} F/m), c is the velocity of light in a vacuum (3 × 10^8 m/s), n_o is the linear refractive index of the sample, n_2 is the nonlinear refractive index, λ is the wavelength of laser beam and β is the nonlinear absorption coefficient. The third order nonlinear optical susceptibility of the pure and 1 mol % of NaCl doped SA crystals were calculated using the relation

$$\chi^{(3)} = \sqrt{\left(R_e\chi^{(3)}\right)^2 + \left(I_e\chi^{(3)}\right)^2} \quad (11)$$

The experimental parameters and calculated results from the Z-scan measurement for pure and 1 mol % of NaCl doped SA crystals are given in Table 2. The calculated nonlinear refractive index (n_2) of grown pure and NaCl doped SA crystals are 5.406× 10^{-11} m^2/W and 5.806× 10^{-11} m^2/W. The positive sign of the nonlinear refractive index (n_2) indicates the self focusing nature of the crystals. This may have an advantage in practical devices, by providing remote sensing and lightning control [45, 46]. From the open aperture Z-scan curve, the nonlinear absorption coefficient (β) is 2.563 × 10^{-4} m/W for pure SA and 2.909 × 10^{-4} m/W for 1 mol % of NaCl doped SA crystal. The positive value of nonlinear coefficient (β) shows the two-photon absorption process. The determined real and imaginary parts of the third order nonlinear susceptibility are 7.256 × 10^{-9} esu, 1.733 × 10^{-7} esu for pure and 8.485 × 10^{-9} esu, 2.142 × 10^{-7} esu for NaCl doped SA crystal respectively. The absolute third order nonlinear optical susceptibility (χ^3) is determined to be 1.735 × 10^{-7} esu for pure and 2.143 × 10^{-7} esu for 1 mol % of NaCl doped SA crystal. The observed results show that the grown NaCl doped SA crystals have higher nonlinear optical susceptibility than Pure SA which reveals that the grown materials are suitable one for non linear optical applications especially for optical limiters and optical modulators.

Table 2
Nonlinear optical parameters of pure and 1 mol % NaCl doped SA crystals.

NLO parameters	Undoped SA	1 mol% NaCl doped SA
Laser beam wavelength (λ)	632.8 nm	632.8 nm
Lens focal length (f)	30 mm	30 mm
Optical bath length	85 cm	85 cm
Beam radius of the aperture (w_a)	3.3 mm	3.3 mm
Aperture radius (r_a)	2 mm	2 mm
Sample thickness (L)	0.59 mm	0.60 mm
Effective thickness (L_{eff})	6.00 × 10^{-4} m	6.00 × 10^{-4} m
Nonlinear refractive index (n_2)	5.406× 10^{-11} m^2/W	5.806× 10^{-11} m^2/W
Nonlinear absorption coefficient (β)	2.563 × 10^{-4} m/W	2.909 × 10^{-4} m/W
Third order nonlinear optical susceptibility (χ^3)	1.735 × 10^{-7} esu	2.143 × 10^{-7} esu

4. Conclusion

Single crystals of pure and 1 mol % of NaCl doped sulphamic acid were grown by a slow evaporation technique. The grown crystals have well defined external appearance. Single crystal and powder X-ray diffraction analysis confirm both pure and 1 mol % of NaCl doped sulphamic acid crystals have orthorhombic system. From EDAX spectrum, it was confirmed the presence of Na^+ ion in SA crystal. The UV-Vis studies show that the grown pure and doped sulphamic acid crystals have no significant absorption in the visible and the transparency is slightly increased by the addition of a dopant. From photoluminescence studies, sharp violet emission peaks observed at 335 nm and 340 nm for pure and doped crystals, respectively. The TGA/DTA studies show that the presence of impurity increases the thermal stability of SA crystals. Vickers microhardness value increases with increasing of applied load and cracks developed for the load above 200 g. The hardening coefficient was found to be 2.018 for pure and 2.233 1 mol % of NaCl doped SA crystal. The photo current and dark current of pure and 1 mol % of NaCl doped SA crystals were increased linearly with the applied voltage. The laser damage threshold value is 27.42, 42.83 and 17.72 GW/cm^2 for pure, NaCl doped SA and KDP crystal respectively. The third order nonlinear optical susceptibility of pure and 1 mol % of NaCl doped SA crystals are 1.735 × 10^{-7} esu, and 2.143 × 10^{-7} esu respectively.

Declarations

Author contribution statement

Selvapandiyan Marimuthu, Arumugam Jemini, Natesan Suresh, Selvakumar Sudhakar, M Prasath: Conceived and designed the experiments; Performed the experiments; Analyzed and interpreted the data; Contributed reagents, materials, analysis tools or data; Wrote the paper.

Funding statement

This research did not receive any specific grant from funding agencies in the public, commercial, or not-for-profit sectors.

Competing interest statement

The authors declare no conflict of interest.

Additional information

No additional information is available for this paper.

Acknowledgements

Authors would like to thank The Head, Department of Physics, St. Joseph College, Trichy for extending the characterization facilities of UV-Visible studies.

References

[1] S. Mary Delphine, A.R.S. Janci Julit, S. Janarthanan, R. Sugaraj Samuel, Study on growth, spectral, optical and thermal characterization of an NLO crystal: 6-methyl nicotinic acid (6MNA), J. Opt. Laser Technol. 90 (2017) 133–135.
[2] D.S. Chemla, J. Zyss, Nonlinear Optical Properties of Organic Molecules and Crystals 1&2, Academic Press, New York, 1987.
[3] B. Singh, M. Shkir, S. AlFaify, A. Kaushal, N. Nasani, I. Bdikin, H. Shoukry, I.S. Yashia, H. Algarni, Structural, optical, thermal, mechanical and dielectric studies of sulfamic acid single crystals: an influence of dysprosium (Dy3+) doping, J. Mol. Struct. 119 (2016) 365–372.
[4] K. Srinivasan, J. Arumugam, Growth of non-linear optical γ-glycine single crystals and their characterization, J. Opt. Mater. 30 (2007) 40–43.
[5] R. Thirumurugan, K. Anitha, Structural, optical, thermal, dielectric, laser damage threshold and Z-scan studies on fumarate salt of creatinine: a promising third-order nonlinear optical material, Mater. Lett. 206 (2017) 30–33.
[6] S. Jeyaram, T. Geethakrishnan, Third-order nonlinear optical properties of acid green 25 dye by Z-scan method, J. Opt. Laser Technol. 89 (2017) 179–185.
[7] M. Mutailipu, M. Zhang, B. Zhang, L. Wang, Z. Yang, X. Zhou, S. Pan, $SrB_5 O_7 F_3$ Functionalized with $[B_5 O_9 F_3]^{6-}$ chromophores: accelerating the rational design of deep-ultraviolet nonlinear optical materials, Angew. Chem. Int. Ed. 57 (2018) 6095–6099.
[8] M. Mutailipu, M. Zhang, H. Wu, Z. Yang, Y. Shen, J. Sun, S. Pan, $Ba_3Mg_3(BO_3)_3F_3$ polymorphs with reversible phase transition and high performances as ultraviolet nonlinear optical materials, Nat. Commun. 9 (2018) 3089–3098.
[9] K. Senthil, S. Kalainathan, Y. Kondo, F. Hamada, M. Yamada, Investigation on the crystal growth, molecular structure and nonlinear optical susceptibilities of 2-[2-(4-ethoxy-phenyl)-vinyl]-1-ethyl-stilbazolium iodide (EESI) by Z-scan technique using He-Ne laser for third-order nonlinear optical applications, J. Opt. Laser Technol. 90 (2017) 242–251.
[10] S.A. Martin Britto Dhass, S. Natarajan, Growth and characterization of Lithium hydrogen oxalate monohydrate, a new semiorganic NLO material, Mater. Lett. 62 (2008) 1136–1138.
[11] C. Gnana Sambandan, S. Perumal, Effect of Mg^{2+} substitution on structural, dielectric, and transport properties of l-tartaric acid-nicotinamide organic crystals, Physica B 405 (2010) 1221–1227.
[12] H. Arul, D. Rajan Babu, R. Ezhilvizhi, G. Bhagavannarayana, Investigation on nucleation kinetics, structural and dielectric properties of an organic NLO single crystal—L-Histidinium maleate (LHM), J. Cryst. Growth 423 (2015) 22–27.
[13] M. Senthilpandiyan, Urit Charoen-In, P. Ramasamy, P. Manyum, M. Lenin, N. Balamurugan, Unidirectional growth of sulphamic acid single crystal and its quality analysis using etching, microhardness, HRXRD, UV-visible and thermogravimetric-differential thermal characterizations, J. Cryst. Growth 312 (2010) 397–401.
[14] R. Valluvan, K. Selvaraju, S. Kumararaman, Growth and characterization of sulphamic acid single crystals: a nonlinear optical material, Mater. Chem. Phys. 97 (2006) 81–84.
[15] R. Ramesh Babu, K. Sethuraman, N. Vijayan, R. Gopalakrishnan, P. Ramasamy, Dielectric and structural studies on sulphamic acid (SA) single crystal, Mater. Lett. 61 (2007) 3480–3485.
[16] R. Ramesh Babu, R. Ramesh, R. Gopalakrishnan, K. Ramamurthi, G. Bhagavannarayana, Growth, structural, spectral, mechanical and optical properties of pure and metal ions doped sulphamic acid single crystals, Spectrochim. Acta Part A Mol. Biomol. Spectrosc. 76 (2010) 470–475.
[17] S. Kalim, A.B. Lad, B.H. Pawar, Dielectric study of KCl doped ADP crystal, J. Chem. Tech. Res. 6 (1) (2014) 206–212.
[18] R. Ramesh Babu, R. Ramesh, R. Gopalakrishnan, K. Ramamurthi, G. Bhagavannarayana, Growth, structural, spectral, mechanical and optical properties of pure and metal ions doped sulphamic acid single crystals, Spectrachim. Acta Part A 76 (2010) 470–475.
[19] B. Brahmaji, S. Rajyalakshmi, Ch Satya Kamal, V. Atla, V. Veeraiah, K. Venkateswara Rao, K. Ramachandra Rao, Optical emissions of Ce^{3+} doped sulphamic acid single crystals by low temperature unidirectional growth technique, Opt. Mater. 64 (2017) 100–105.
[20] T. Thaila, S. Kumararaman, Effect of NaCl and KCl doping on the growth of sulphamic acid crystals, Spectrachim. Act Part A 82 (2011) 20–24.
[21] P. Rajesh, P. Ramasamy, B. Kumar, G. Bhagavannarayana, Effect of cobalt and dl-malic acid on the growth rate, crystalline perfection, optical, mechanical, dielectric, piezoelectric properties and SHG efficiency of ADP single crystals, Physica B 405 (2010) 2401–2406.
[22] M. Mutailipu, Z. Xie, X. Su, M. Zhang, Y. Wang, Z. Yang, M.A. Janjua, S. Pan, Chemical cosubstitution-oriented design of rare-earth borates as potential ultraviolet nonlinear optical materials, J. Am. Chem. Soc. 139 (2017) 18397–18405.
[23] P.V. Dhanaraj, N.P. Rajesh, Growth and characterization of nonlinear optical γ-glycine single crystal from lithium acetate as solvent, Mater. Chem. Phys. 115 (2009) 413–417.
[24] P. Muthusubramanian, A. Sundara Raj, Internal modes and normal coordinate analysis of sulphamic acid, J. Mol. Struct. 84 (1982) 25–37.
[25] N. Rani, N. Vijayan, Kanika Thukral, K.K. Maurya, D. Haranath, G. Bhagavannarayana, S. Verma, M.A. Wahab, Crystalline perfection, optical and third harmonic generation analyses of non-linear optical single crystal of L-lysine acetate, Spectrochim. Acta Part A Mol. Biomol. Spectrosc. 105 (2013) 192–199.
[26] S. Sakthy Priya, A. Alexandar, P. Surendran, A. Lakshmanan, P. Rameskumar, P. Sagayaraj, Investigations on nucleation, HRXRD, optical, piezoelectric, polarizability and Z-scan analysis of l–arginine maleate dihydrate single crystals, Opt. Mater. 66 (2017) 434–441.
[27] H.G. Kuball, T. Hofer, S. Kiesewalter, Chiroptical Spectroscopy: General Theory, Academic Press, Germany, 1999.
[28] J.E. House, Fundamental of Quantum Mechanics, third ed., Academic Press, USA, 2018.
[29] N. Vijayan, G. Bhagavannarayana, R. Ramesh Babu, R. Gopalakrishnan, K.K. Maurya, P. Ramasamy, A comparative study on solution- and bridgman-grown single crystals of benzimidazole by high-resolution X-ray diffractometry, fourier transform infrared, microhardness, laser damage threshold, and second-harmonic generation measurements, Cryst. Growth Des. 6 (2006) 1542.
[30] N. Pattanaboommee, P. Ramasamy, R. Yimnirum, A comparative study on pure, l-arginine and glycine doped ammonium dihydrogen orthophosphate single crystals grown by slow solvent evaporation and temperature-gradient method, J. Cryst. Growth 314 (2011) 196–201.
[31] P. Rajesh, P. Ramasamy, A study on optical, thermal, mechanical, dielectric, piezoelectric and NLO properties of unidirectional ammonium chloride added ammonium dihydrogen phosphate crystal, Mater. Lett. 63 (2009) 2260–2262.
[32] K. Boopathi, P. Rajesh, P. Ramasamy, Growth of negative solubility lithium sulfate monohydrate crystal by slow evaporation and Sankaranarayanan–Ramasamy method, J. Cryst. Growth 345 (2012) 1–6.
[33] M.K. Marchewka, S. Debrus, H. Ratajczak, Vibrational spectra and second harmonic generation in molecular complexes of l-lysine with l-tartaric, d,l-malic, acetic, arsenous, and fumaric acids, Cryst. Growth Des. 3 (2003) 587–592.
[34] M. Selvapandiyan, J. Arumugam, P. Sundaramoorthi, S. Sudhakar, Influence of $MgSO_4$ doping on the properties of zinc tris–thiourea sulphate (ZTS) single crystals, J. Alloys Compd. 580 (2013) 270–275.
[35] E.M. Onitsch, U ber die Mikroharte der Metalle, Mikroscopia 2 (1947) 131–151.
[36] C. Senthikumar, R. Jagan, P. Rajesh, P. Ramasamy, Spectral, mechanical, thermal, optical and solid state parameters, of metal-organic bis(hydrogenmaleate)-CO(II) tetrahydrate crystal, J. Solid State Chem. 230 (2015) 135–142.
[37] G. Saravanakumar, P. Vivek, P. Murugakoothan, A combined experimental and quantum chemical analysis to explore the nonlinear optical activity of guanidinium l-monohydrogen tartrate, Spectrochim. Acta Part A Mol. Biomol. Spectrosc. 145 (2015) 417–424.
[38] K. Nivetha, S. Kalainathan, M. Yamada, Y. Kondo, F. Hamada, Synthesis, growth, and characterization of new stilbazolium derivative single crystal: 2-[2-(2,4-dimethoxy-phenyl)-vinyl]-1-ethyl-pyridinium iodide for third-order NLO applications, J. Mater. Chem. Phys. Mater. Electron. 28 (2017) 5180–5191.
[39] P. Karuppusamy, M.S. Pandiyan, P. Ramasamy, S. Verma, Crystal growth, structural, optical, thermal, mechanical, laser damage threshold and electrical properties of triphenylphosphine oxide 4-nitrophenol (TP4N) single crystals for nonlinear optical applications, Opt. Mater. 79 (2018) 152–171.
[40] R.M. Wood, Laser-induced Damage of Optical Materials, Institute of Physics Publishing, Dirac House, Bristol, UK, 2003.
[41] M. Sheik-Bahae, A.A. Said, T. Wei, D.J. Hagan, E.W. Van Stryland, Sensitive measurement of optical nonlinearities using a single beam, IEEE J. Quant. Electron. 26 (1990) 760–769.
[42] M. Sheik-Bahae, A.A. Said, E.W. Van Stryland, High-sensitivity, single-beam n_2 measurements, Opt. Lett. 14 (1989) 955–957.
[43] M.C. Sreenath, I. Hubert Joe, V.K. Rastogi, Experimental and theoretical investigation of third-order nonlinear optical properties of azo dye 1-(2, 5-dimethoxy-phenylazo)-naphthalen-2-ol by Z-scan technique and quantum chemical computations, Dyes Pigments 157 (2018) 163–178.
[44] Y. Eranade, M.C. Sreenath, S. Chitrambalam, I.S. Joe, N. Sekar, Spectroscopic, DFT and Z-scan supported investigation of dicyanoisophorone based push-pull NLOphoric styryl dyes, Opt. Mater. 66 (2017) 494–511.
[45] P. Karuppusamy, T. Kamalesh, K. Anitha, S.A. Kalam, M.S. Pandiyan, P. Ramasamy, S. Verma, S. Venugopal Rao, Synthesis, crystal growth, structure and characterization of a novel third order nonlinear optical organic single crystal: 2-amino 4,6-dimethyl pyrimidine 4-nitrophenol, Opt. Mater. 84 (2018) 475–489.
[46] K. Senthil, S. Kalainathan, F. Hamada, M. Yamada, P.G. Aravindan, Synthesis, growth, structural and HOMO and LUMO, MEP analysis of a new stilbazolium derivative crystal: a enhanced third-order NLO properties with a high laser-induced damage threshold for NLO applications, Opt. Mater. 46 (2015) 565–577.